

Cupric chloride CuCl_2 as an $S=\frac{1}{2}$ chain multiferroic

S. Seki,¹ T. Kurumaji,¹ S. Ishiwata,^{1,2} H. Matsui,^{3,4} H. Murakawa,⁵ Y. Tokunaga,⁵ Y. Kaneko,⁵ T. Hasegawa,⁴ and Y. Tokura^{1,2,5}

¹Department of Applied Physics, University of Tokyo, Tokyo 113-8656, Japan

²Cross-Correlated Materials Research Group (CMRG) and Correlated Electron Research Group (CERG), RIKEN Advanced Science Institute, Wako 351-0198, Japan

³Department of Advanced Materials Science, The University of Tokyo, Kashiwa 277-8561, Japan

⁴Photonics Research Institute (PRI), AIST, Tsukuba 305-8562, Japan

⁵Multiferroics Project, ERATO, Japan Science and Technology Agency (JST), Tokyo 113-8656, Japan

(Received 21 June 2010; revised manuscript received 10 August 2010; published 30 August 2010)

Magnetolectric properties were investigated for an $S=1/2$ chain antiferromagnet CuCl_2 , which turns out to be the first example of nonchalcogen based spiral-spin induced multiferroics. Upon the onset of helimagnetic order propagating along the b axis under zero magnetic field (H), we found emergence of ferroelectric polarization along the c axis. Application of H along the b axis leads to spin-flop transition coupled with drastic suppression of ferroelectricity and rotation of H around the b axis induces the rotation of spin-spiral plane and associated polarization direction. These behaviors are explained well within the framework of the inverse Dzyaloshinskii-Moriya model, suggesting the robustness of this magnetolectric coupling mechanism even under the strong quantum fluctuation.

DOI: [10.1103/PhysRevB.82.064424](https://doi.org/10.1103/PhysRevB.82.064424)

PACS number(s): 75.85.+t, 75.10.Pq, 75.45.+j, 77.80.Fm

I. INTRODUCTION

Multiferroics, materials with both magnetic and dielectric orders, have attracted revived interest.¹ While the coupling between these orders are weak in general, recent discovery of spin-driven ferroelectricity in frustrated helimagnets has enabled unprecedentedly large magnetolectric (ME) effects such as flop,^{2–4} reversal,⁵ or rotation⁶ of electric polarization (P) under applied magnetic field (H). Here, the key problem is the coupling mechanism between ferroelectricity and helimagnetism. The most successful scheme to explain such ME coupling is the inverse Dzyaloshinskii-Moriya (IDM) model,⁷ which describes the local polarization \vec{p}_{ij} produced between two magnetic moments \vec{S}_i and \vec{S}_j as

$$\vec{p}_{ij} = A\vec{e}_{ij} \times (\vec{S}_i \times \vec{S}_j), \quad (1)$$

where \vec{e}_{ij} is an unit vector connecting two magnetic sites and A is a coupling coefficient related to the spin-orbit interaction. Since the vector spin chirality ($\vec{S}_i \times \vec{S}_j$) is perpendicular to the spin-spiral plane, this model predicts that the H -induced tilt of spin-spiral plane leads to directional change of P . Ferroelectric (FE) and ME natures in several classical helimagnets such as RMnO_3 ,^{2,3} $\text{Ni}_3\text{V}_2\text{O}_8$,⁸ and MnWO_4 (Ref. 4) are successfully explained by this IDM scheme.

In contrast, still in controversy is the ME coupling mechanism in $S=1/2$ chain magnets, where strong quantum fluctuation is believed to have some profound effects on their ME response.^{9,10} Typical examples are LiCu_2O_2 and LiCuVO_4 , both of which are characterized by edge-shared CuO_2 chains. While their simple crystal structures and reported helimagnetism are seemingly typical of the IDM scheme, the experimentally observed P direction or ME response for applied H appears to contradict with its prediction. For example, LiCu_2O_2 hosts $P\parallel c$ in the helimagnetic ground state¹¹ but its proposed magnetic structures are contradictory among several experiments.^{12–15} Even if we sim-

ply assume bc -spin spiral consistent with the IDM model, P behaviors under applied H contradict with its naive prediction.¹¹ In case of LiCuVO_4 , $P\parallel a$ is found in ab -spiral spin phase at 0 T, consistent with the IDM model.^{16,17} However, the observation of $P\parallel c$, assigned to the bc -spiral spin phase,¹⁸ was not reproduced by another group.¹⁹ Since both compounds frequently contains Li-Cu intersubstitution due to their close ionic radii, Moskvina *et al.*^{20–22} have claimed that the observed FE and ME natures stem purely from exchange striction and crystallographic defects, not from the spin-orbit interaction (or the IDM scheme). Furthermore, some recent theoretical study predicted that quantum fluctuation may largely reduce the effective magnitude of P induced via the spin-orbit interaction.¹⁰ To testify the validity of the IDM model in quantum chain magnets, it is crucial to check the ME response in other $S=1/2$ compounds with similar edge-shared chain structures.

Our target compound, anhydrous cupric chloride CuCl_2 crystallizes into distorted CdI_2 form with monoclinic $C2/m$ space group and $\beta=122^\circ$.²³ While original CdI_2 structure consists of the stacking of triangular lattices along the z axis,²⁴ they are extended along the a axis due to Jahn-Teller active Cu^{2+} ions [Fig. 1(a)]. As a result, CuCl_2 can be regarded as the aggregate of edge-shared chains running along the b axis with CuCl_4 square plaquettes lying in the bc plane [Fig. 1(b)]. Magnetism is dominated by the intrachain coupling between Cu^{2+} ($S=1/2$) ions, and competition between ferromagnetic nearest-neighbor interaction and antiferromagnetic next-nearest-neighbor interaction stabilizes the helimagnetic ground state below 24 K.^{25–27} Recent powder neutron scattering study suggested the cycloidal magnetic order propagating along the b axis with spin spiral confined in the bc plane [Fig. 1(b)] and propagation vector $q \sim (1, 0.226, 0.5)$.²⁷ While no dielectric measurements have been reported, the latest calculation based on density-functional theory (DFT) predicts emergence of ferroelectric-

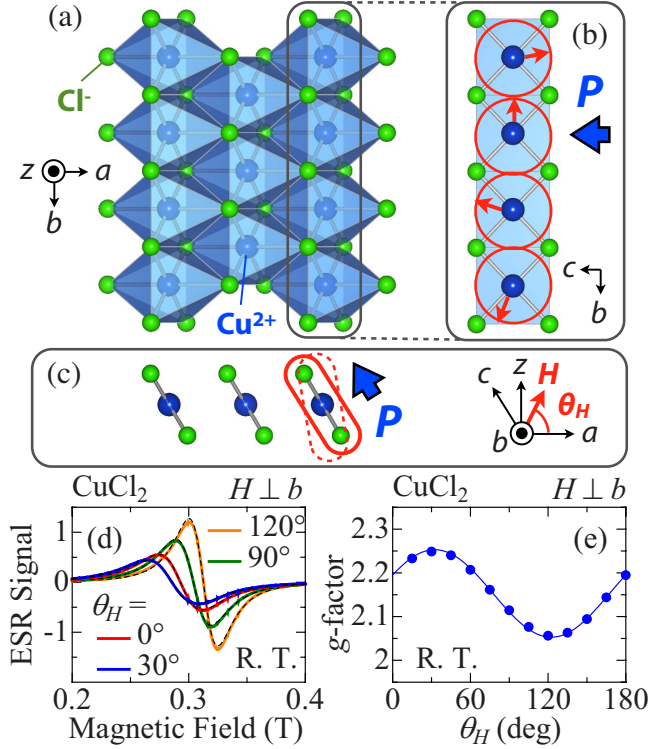


FIG. 1. (Color online) [(a)–(c)] Crystal structure of CuCl_2 , and P direction observed at the ground state. The bc -cycloidal spin order suggested by Banks *et al.* (Ref. 27) is illustrated in (b) and also in (c) with solid rounded square representing spin-spiral plane. Dashed rounded square indicates the possible tilting of spin-spiral plane as revealed in this study (see text). (d) ESR signal taken at room temperature under various directions of H confined within the ac plane. θ_H is defined as the angle between the a axis and H direction. Each dashed line represents a fitted curve with a single Lorentzian resonance. (e) Angle dependence of g factor.

ity along the c axis.²⁷ In this paper, we report the experimental discovery of FE and ME natures in CuCl_2 , and prove that the IDM mechanism is still robust even under the strong quantum fluctuation. CuCl_2 is a rare example of nonchalcogen-based spiral-spin-induced multiferroics, which promises further discovery of unique ME function in many MX_2 -type compounds and other forms of halide compounds.

II. EXPERIMENT

Single crystals of CuCl_2 were grown by a Bridgman method. They were cleaved along planes perpendicular to the z axis and cut into a rectangular shape with additional faces perpendicular to the a or b axis. Silver paste was painted on end surfaces as electrodes. Due to its moisture sensitivity, the specimen was handled in an Ar-filled glove box. To deduce P , we measured the polarization current with constant rates of temperature (T) sweep (5–20 K/min), H sweep (100 Oe/sec), or H rotation (2° /sec), and integrated it with time. To enlarge the population of specific P domain, the poling electric field ($E=150$ – 400 kV/m) was applied in the cooling process and removed just prior to the measurements of polarization current. Dielectric constant ϵ was measured at 1

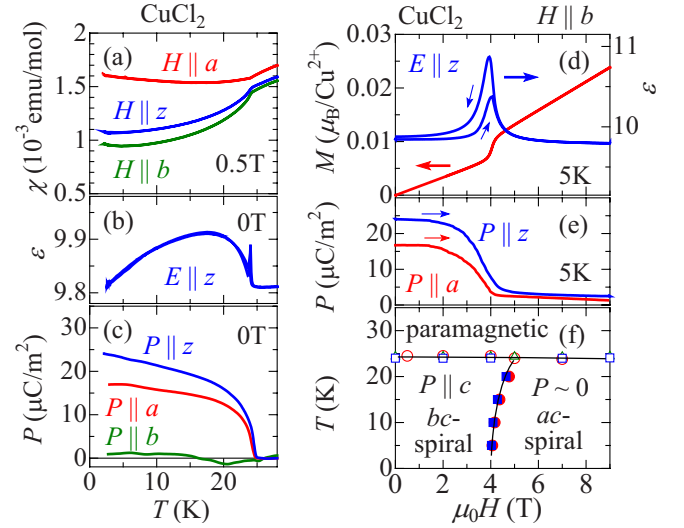


FIG. 2. (Color online) Temperature dependence of (a) magnetic susceptibility χ , (b) dielectric constant ϵ , and (c) electric polarization P . In (d) and (e), H dependences of magnetization M , ϵ , and P under $H \parallel b$ are indicated. Large and small arrows denote corresponding ordinate scale of physical quantity and direction of field scans, respectively. (f) H - T phase diagram for $H \parallel b$. Circles, squares, triangles are the data points obtained from M , ϵ , and P profiles, respectively. Open (closed) symbols are taken from T - (H) increasing runs.

MHz using LCR meter. Magnetization M was measured with a superconducting quantum interference device magnetometer. Electron spin resonance (ESR) signal was measured by JEOL JES-FA200 at X-band frequency (~ 9.0 GHz).

III. RESULTS AND DISCUSSIONS

As suggested in Ref. 27, the ac -twin domains are expected to readily occur. To check this possibility, we first performed ESR measurements under various directions of H confined within the ac plane [Fig. 1(d)]. Hereafter, we define θ_H as the angle between the a axis and H direction. Each observed profile can be fitted well with a single Lorentzian resonance for all θ_H , indicating our crystal grown by the Bridgman method has no crystallographic twinning. The deduced g factor shows sinusoidal θ_H dependence [Fig. 1(e)], whose maximum and minimum values agree well with those previously reported for a twinned crystal.²⁷

Next, we measured T dependence of magnetic susceptibility χ , ϵ , and P [Figs. 2(a)–2(c)]. χ suddenly drops at $T_N \sim 24$ K, which signals the transition into a spiral magnetic phase. Simultaneously, z component of ϵ (ϵ_z) shows a sharp anomaly, and a and z components of P (P_a and P_z) begin to develop. The direction of P_z can be reversed with reversal of applied E , producing the typical P - E hysteresis curve (Fig. 3), while no P_b component could be confirmed. These results imply strong correlation between helimagnetic and FE orders in CuCl_2 . Based on the bc -plane helimagnetic structure suggested in Ref. 27, the IDM model as well as the DFT calculation²⁷ predicts $|P_a/P_z| \sim 0.64$ (i.e., $P \parallel c$). This roughly agrees with the observed $|P_a/P_z| \sim 0.70$.

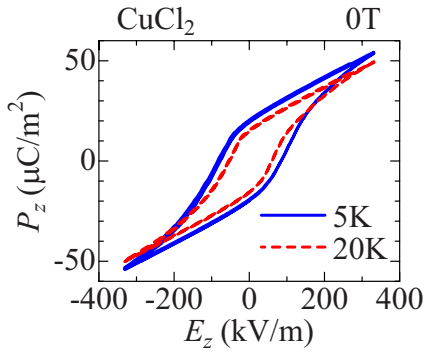


FIG. 3. (Color online) P - E hysteresis loop for CuCl_2 measured with $E \parallel z$. Electric field was swept at the rate of 13 kV/m sec.

Figures 2(d) and 2(e) indicate H dependence of M , ϵ , and P for $H \parallel b$. At 4 T, M profile shows a clear step as already reported.^{27,28} Concomitantly, ϵ_z shows a sharp peak and both P_a and P_z are drastically suppressed. Since antiferromagnetic spins favor to lie within a plane perpendicular to H , this transition should correspond to a spin flop into the ac -spiral spin state. The ac -spiral spin structure belongs to a magnetic form called proper screw, where spin-spiral plane is perpendicular to the modulation vector along the b axis. The IDM model predicts $P=0$ for this type of spin order due to the relationship $(\vec{S}_i \times \vec{S}_j) \parallel \vec{e}_{ij} \parallel b$, which is consistent with the observed suppression of P . Figure 2(f) summarizes the obtained H - T phase diagram for $H \parallel b$. The boundary of the FE phase always coincides with that for magnetic phases, which proves the interplay between FE and helimagnetic natures.

We further investigated the properties under $H \perp b$. Here, we adopt the same definition of θ_H as used for ESR measurements. Figure 4(a) indicates H dependence of M measured at various θ_H . While no magnetic transition has been reported for $H \perp b$,²⁸ we found a clear signature of spin-flop at $H_{\text{SF}} \sim 4$ T most pronounced around $\theta_H = 100^\circ$. θ_H dependence of $\chi (=M/H)$ was also measured [Fig. 4(b)], and χ sinusoidally changes with minimum at $\theta_H \sim 100^\circ$ below H_{SF} . In general, the sharpest transition of spin flop as well as the minimum value of χ should be observed when H is applied parallel to the magnetic easy plane. These results imply the magnetic easy plane, i.e. spin-spiral plane at the ground state, is tilted from the originally suggested bc plane toward the bz plane by about 20° [Fig. 1(c)]. Above H_{SF} , χ still modulates sinusoidally but with different χ -minimum position at $\theta_H \sim 122^\circ$ (i.e., $H \parallel c$). With $H > H_{\text{SF}}$, the gain of Zeeman energy exceeds the energy loss due to magnetic anisotropy, and continuous rotation of spin-spiral plane is expected. In this case, θ_H dependence of χ rather reflects the anisotropy of g value,²⁹ whose minimum is also confirmed to appear at $H \parallel c$ [Fig. 1(e)].

To investigate the behavior of P under H rotating around the b axis, we simultaneously measured P_z and P_a using two pairs of electrodes. Thus, both P and H can be expressed as vectors within the ac plane. We also define θ_p as the angle between the a axis and observed P direction [Fig. 5(d)]. Figures 4(d) and 4(e) indicate θ_H dependences of P_z and P_a measured at 5 T. When H is rotated by 180° , P direction is always found to be reversed. To see the behavior of P more

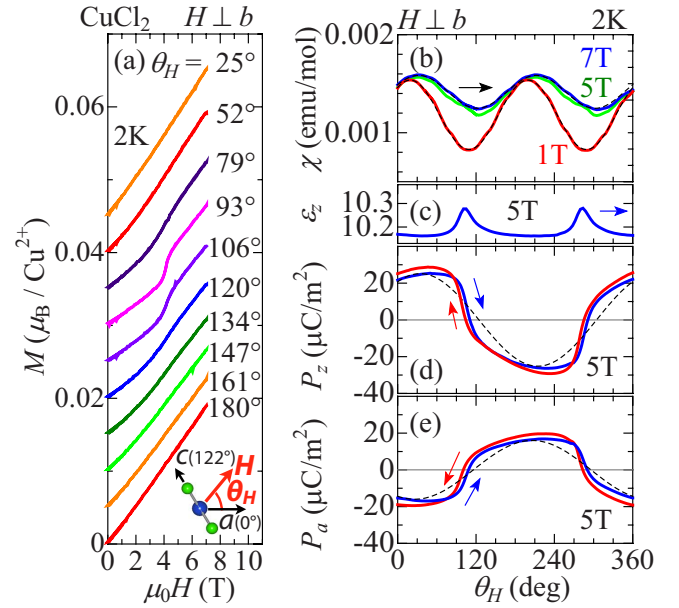


FIG. 4. (Color online) (a) H dependence of M taken under various directions of H around the b axis. The base lines of data are arbitrarily shifted. (b) Angle dependence of χ measured under $H \perp b$. Dashed lines indicate the fits with sinusoidal function. [(c)–(e)] Corresponding development of z component of ϵ (ϵ_z) as well as z and a components of P (P_z and P_a). Before measurements of P , the specimen was cooled at $\theta_H = 0$ with poling E applied along the z axis. Dashed lines indicate the behavior expected from Eq. (2). Arrows indicate the direction of H rotation.

straightforwardly, the trace of P is plotted in the P_a - P_z plane [Fig. 5(a)]. It forms a shape like elongated ellipse. In Figs. 5(b) and 5(c), θ_H dependences of $|P|$ (magnitude of \vec{P}) and θ_p are indicated. θ_p takes almost constant value around $\theta_p = 120^\circ$ or 300° , suggesting the major axis of observed P ellipse is pointing at the c axis. If we assume that H is always perpendicular to the spin-spiral plane, i.e., $\vec{H} \parallel (\vec{S}_i \times \vec{S}_j)$, the IDM model predicts $\vec{P} = \vec{P}_1 \parallel c$ for $\vec{H} \perp c$ [Fig. 5(e)] and $\vec{P} = \vec{P}_2 \perp c$ for $\vec{H} \parallel c$ [Fig. 5(f)]. For general θ_H , \vec{P} is given as

$$\vec{P} = \vec{P}_1 \sin(122^\circ - \theta_H) + \vec{P}_2 \cos(122^\circ - \theta_H), \quad (2)$$

which forms an ellipse-shaped trace with \vec{P}_1 and \vec{P}_2 as the major and minor axes, respectively. From the $|P|$ profile, we deduced $|\vec{P}_1| \sim 31 \mu\text{C}/\text{m}^2$ and $|\vec{P}_2| \sim 2 \mu\text{C}/\text{m}^2$.

In Figs. 4(d) and 4(e), the P behavior expected from Eq. (2) is plotted as dashed lines. While the calculated P profile roughly agrees with the observed one, small gap still exists between them. This deviation reverses its sign at $\theta_H \sim 100^\circ$, where H becomes parallel to the magnetic easy plane. Correspondingly, ϵ also shows small anomaly at $\theta_H \sim 100^\circ$ [Fig. 4(c)]. These behaviors can be well explained by assuming that the spin-spiral plane is tilted from the originally expected $\vec{H} \parallel (\vec{S}_i \times \vec{S}_j)$ position toward the magnetic easy plane. A similar effect of magnetic-anisotropy drag on P has also been observed in the H -rotating experiment on $\text{Eu}_{1-x}\text{Y}_x\text{MnO}_3$.⁶

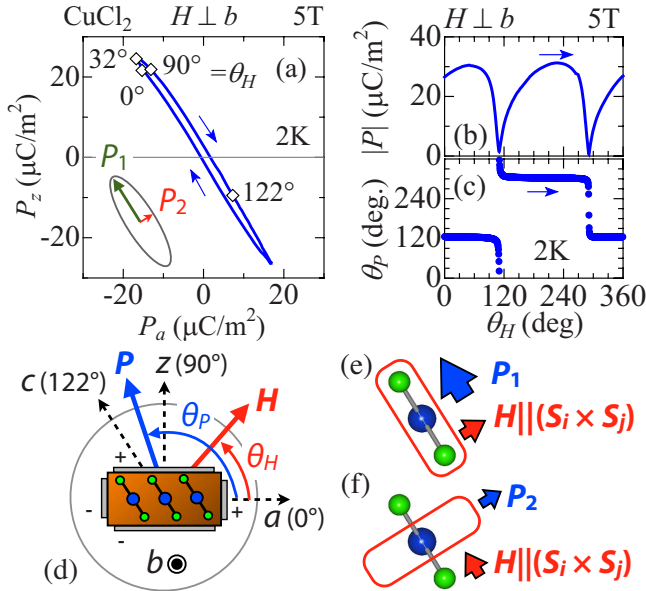


FIG. 5. (Color online) (a) Trace of P_a and P_z under H rotating around the b axis. [(b) and (c)] Magnitude and direction of P as a function of H angle. Arrows indicate the direction of H rotation. The data are taken from Figs. 4(d) and 4(e), and the setup for measurements is shown in (d). θ_p (θ_H) is defined as the angle between P (H) direction and the a axis. [(e) and (f)] The expected relationship between P , H , and spin-spiral plane (depicted as rounded square).

Thus, we conclude that the IDM scheme can well reproduce the observed FE and ME natures, even for CuCl_2 with $S=1/2$ quantum spin chains. Note that $P \parallel c$ relationship observed at 0 T can be justified even with a slight revision of the originally suggested bc -spiral spin structure since deduced ratio $|\vec{P}_1|/|\vec{P}_2| \sim 15$ is quite large. Notably, when H and spin-spiral plane is rotated counterclockwise, P is found to rotate clockwise [Fig. 5(a)]. This is in contrast with the case for $\text{Eu}_{1-x}\text{Y}_x\text{MnO}_3$,⁶ where both H and P rotate in the same direction. The observed manner of P rotation and large $|\vec{P}_1|/|\vec{P}_2|$ ratio are in accord with the recent DFT calculation for edge-shared CuO_2 chain compounds,³⁰ and these features would reflect the anisotropy and sign of coupling coefficient A in Eq. (1).

CuCl_2 is also the first example of nonchalcogen-based spiral-spin-induced multiferroics. While observed $|\vec{P}_1| \sim 31 \mu\text{C}/\text{m}^2$ is somewhat smaller than the calculation

($|\vec{P}_1| \sim 84 \mu\text{C}/\text{m}^2$),²⁷ it is comparable with the case for other helimagnetic oxides ($2000\text{--}5 \mu\text{C}/\text{m}^2$). Interestingly, a recent theoretical study suggested the choice of anion may largely affect the value of induced P through the different strength of metal-ligand hybridization and spin-orbit coupling.³¹ This means that the ME response can be enhanced if we choose appropriate anion as the ligand. Until now, the study of ferroelectric helimagnets is almost limited to oxides, partly because their isostructural chalcogen relatives with larger anions (i.e., sulfides or selenides) are often electrically too leaky to perform dielectric measurements.^{32–34} Since halogens have larger electronegativity than chalcogens, halides are better insulating and enable the investigation of ME properties for a wider variety of anions. For example, most of MX_2 -type halides with $X=\text{Cl}$, Br , and I consist of stacking of undistorted triangular lattices, which realizes various types of spiral spin orders.^{35–37} The systematic investigation of FE properties of whole MX_2 system will offer a good opportunity to clarify the anion dependence of magnetically induced ferroelectricity, which may contribute to a general strategy to obtain larger ME responses.

IV. CONCLUSIONS

In summary, we have experimentally revealed magnetically driven ferroelectricity in an $S=1/2$ chain helimagnet CuCl_2 . Observed P behaviors under applied H can be reproduced well within the framework of the inverse Dzyaloshinskii-Moriya model, suggesting the robustness of this ME coupling mechanism even under the effect of strong quantum fluctuation. CuCl_2 is a rare example of nonchalcogen-based spiral-spin-induced multiferroics, which promises further discovery of unique magnetoelectric function in many MX_2 -type compounds and other forms of halide compounds.

ACKNOWLEDGMENTS

The authors thank T. Arima, N. Nagaosa, Y. Kohara, and Y. Taguchi for enlightening discussions. This work was partly supported by MEXT of Japan and JSPS through Grants-In-Aid for Scientific Research (Grants No. 20340086 and No. 2010458) and Funding Program for World-Leading Innovative R&D on Science and Technology (FIRST Program).

¹M. Fiebig, *J. Phys. D* **38**, R123 (2005); S. W. Cheong and M. Mostovoy, *Nature Mater.* **6**, 13 (2007); Y. Tokura and S. Seki, *Adv. Mater.* **22**, 1554 (2010).

²T. Kimura, T. Goto, H. Shintani, K. Ishizaka, T. Arima, and Y. Tokura, *Nature (London)* **426**, 55 (2003).

³T. Goto, T. Kimura, G. Lawes, A. P. Ramirez, and Y. Tokura, *Phys. Rev. Lett.* **92**, 257201 (2004).

⁴K. Taniguchi, N. Abe, T. Takenobu, Y. Iwasa, and T. Arima,

Phys. Rev. Lett. **97**, 097203 (2006).

⁵N. Abe, K. Taniguchi, S. Ohtani, T. Takenobu, Y. Iwasa, and T. Arima, *Phys. Rev. Lett.* **99**, 227206 (2007).

⁶H. Murakawa, Y. Onose, F. Kagawa, S. Ishiwata, Y. Kaneko, and Y. Tokura, *Phys. Rev. Lett.* **101**, 197207 (2008).

⁷H. Katsura, N. Nagaosa, and A. V. Balatsky, *Phys. Rev. Lett.* **95**, 057205 (2005); M. Mostovoy, *ibid.* **96**, 067601(2006); I. A. Sergienko and E. Dagotto, *Phys. Rev. B* **73**, 094434 (2006).

- ⁸G. Lawes, A. B. Harris, T. Kimura, N. Rogado, R. J. Cava, A. Aharony, O. Entin-Wohlman, T. Yildirim, M. Kenzelmann, C. Broholm, and A. P. Ramirez, *Phys. Rev. Lett.* **95**, 087205 (2005).
- ⁹H. Katsura, S. Onoda, J. H. Han, and N. Nagaosa, *Phys. Rev. Lett.* **101**, 187207 (2008).
- ¹⁰S. Furukawa, M. Sato, Y. Saiga, and S. Onoda, *J. Phys. Soc. Jpn.* **77**, 123712 (2008).
- ¹¹S. Park, Y. J. Choi, C. L. Zhang, and S.-W. Cheong, *Phys. Rev. Lett.* **98**, 057601 (2007).
- ¹²T. Masuda, A. Zheludev, A. Bush, M. Markina, and A. Vasiliev, *Phys. Rev. Lett.* **92**, 177201 (2004).
- ¹³S. Seki, Y. Yamasaki, M. Soda, M. Matsuura, K. Hirota, and Y. Tokura, *Phys. Rev. Lett.* **100**, 127201 (2008).
- ¹⁴A. Russydi, I. Mahns, S. Müller, M. Rübhausen, S. Park, Y. J. Choi, C. L. Zhang, S.-W. Cheong, S. Smadici, P. Abbamonte, M. v. Zimmermann, and G. A. Sawatzky, *Appl. Phys. Lett.* **92**, 262506 (2008).
- ¹⁵Y. Kobayashi, K. Sato, Y. Yasui, T. Moyoshi, M. Sato, and K. Kakurai, *J. Phys. Soc. Jpn.* **78**, 084721 (2009).
- ¹⁶Y. Naito, K. Sato, Y. Yasui, Y. Kobayashi, Y. Kobayashi, and M. Sato, *J. Phys. Soc. Jpn.* **76**, 023708 (2007).
- ¹⁷B. J. Gibson, R. K. Kremer, A. V. Prokofiev, W. Assmus, and G. J. McIntyre, *Physica B* **350**, E253 (2004).
- ¹⁸F. Schrettle, S. Krohns, P. Lunkenheimer, J. Hemberger, N. Büttgen, H.-A. Krug von Nidda, A. V. Prokofiev, and A. Loidl, *Phys. Rev. B* **77**, 144101 (2008).
- ¹⁹Y. Yasui, Y. Naito, K. Sato, T. Moyoshi, M. Sato, and K. Kakurai, *J. Phys. Soc. Jpn.* **77**, 023712 (2008).
- ²⁰A. S. Moskvin and S.-L. Drechsler, *Phys. Rev. B* **78**, 024102 (2008).
- ²¹A. S. Moskvin and S.-L. Drechsler, *EPL* **81**, 57004 (2008).
- ²²A. S. Moskvin, Y. D. Panov, and S.-L. Drechsler, *Phys. Rev. B* **79**, 104112 (2009).
- ²³A. F. Wells, *J. Chem. Soc.* **1947**, 1670.
- ²⁴For simplicity, hereafter we define the z axis as the direction perpendicular to both a and b axes [Fig. 1(c)].
- ²⁵J. W. Stout and R. C. Chisholm, *J. Chem. Phys.* **36**, 979 (1962).
- ²⁶M. Schmitt, O. Janson, M. Schmidt, S. Hoffmann, W. Schnelle, S.-L. Drechsler, and H. Rosner, *Phys. Rev. B* **79**, 245119 (2009).
- ²⁷M. G. Banks, R. K. Kremer, C. Hoch, A. Simon, B. Ouladdiaf, J.-M. Broto, H. Rakoto, C. Lee, and M.-H. Whangbo, *Phys. Rev. B* **80**, 024404 (2009).
- ²⁸D. Billerey and C. Terrier, *Phys. Lett. A* **68**, 278 (1978).
- ²⁹T. Nagamiya, *Solid State Phys.* **20**, 305 (1967).
- ³⁰H. J. Xiang and M.-H. Whangbo, *Phys. Rev. Lett.* **99**, 257203 (2007).
- ³¹C. Jia, S. Onoda, N. Nagaosa, and J. H. Han, *Phys. Rev. B* **76**, 144424 (2007).
- ³²S. Seki, Y. Onose, and Y. Tokura, *Phys. Rev. Lett.* **101**, 067204 (2008).
- ³³K. Singh, A. Maignan, C. Martin, and Ch. Simon, *Chem. Mater.* **21**, 5007 (2009).
- ³⁴J. Hemberger, P. Lunkenheimer, R. Fichtl, H.-A. Krug von Nidda, V. Tsurkan, and A. Loidl, *Nature (London)* **434**, 364 (2005); G. Catalan and J. F. Scott, *ibid.* **448**, E4 (2007).
- ³⁵K. Hirakawa, H. Kadowaki, and K. Ubukoshi, *J. Phys. Soc. Jpn.* **52**, 1814 (1983).
- ³⁶J. W. Cable, M. K. Wilkinson, E. O. Wollan, and W. C. Koehler, *Phys. Rev.* **125**, 1860 (1962).
- ³⁷S. R. Kuindersma, J. P. Sanchez, and C. Haas, *Physica B* **111**, 231 (1981).